International Journal of Microwave and Wireless Technologies

cambridge.org/mrf

Experimental validation of an isoflux Earth coverage with a bimode ARMA antenna on a nanosatellite

E. Arnaud[1], A. Siblini[2], A. Bellion[3] and B. Jecko[1]

[1]XLIM – CNRS, 123 Avenue Albert Thomas, 87060 Limoges Cedex, France; [2]Lebanese University, Doctoral School of Technology, Beyrouth, Lebanon and [3]CNES, 18 avenue Edouard Belin, 31401-Toulouse, France

Research Paper

Cite this article: Arnaud E, Siblini A, Bellion A, Jecko B (2020). Experimental validation of an isoflux Earth coverage with a bimode ARMA antenna on a nanosatellite. *International Journal of Microwave and Wireless Technologies* **12**, 66–74. https://doi.org/10.1017/S1759078719001004

Received: 26 October 2018
Revised: 24 June 2019
Accepted: 28 June 2019
First published online: 25 July 2019

Key words:
Agile Radiating Matrix Antenna; circular polarization; isoflux radiation pattern; nanosatellite application

Author for correspondence:
E. Arnaud, E-mail: eric.arnaud@xlim.fr

Abstract

Spatial telemetry links on nanosatellites require more and more reconfigurable beam antennas to improve the Earth coverage. The bi-mode Agile Radiating Matrix Antenna (8.0–8.4 GHz) was successfully designed to solve such kind of problems by using an isoflux mode associated with a switchable directive one. However, such an antenna introduces some manufacturing problems *for the isoflux mode*, mainly due to the small available volume on the nanosatellite platform. This paper describes a solution to this problem thanks to the ARMA concept. A comparison between theoretical and experimental results for the isoflux mode in circular polarization is presented to validate the results.

Introduction

Future nanosatellite missions, especially with LEO satellites, require a wide-angle Earth coverage with a long-time visibility, implying an isoflux radiation pattern called "isoflux mode". Furthermore, this pattern is usually associated with a directive beam ("directive mode") to maintain the gain around the axial direction (nadir). Usually, the choke horn antenna is a good candidate to perform an isoflux radiation pattern [1–6]. Unfortunately, its physical size is not compliant with a nanosatellite application and the bi-mode radiation is not achievable. Planar solutions like patch array antennas [7–12] are interesting but they often suffer from large dimensions to obtain a directive pattern relatively to the platform size. To overcome these limitations, the proposed solution generates both beams by using a new agile low profile antenna called "Agile Radiating Matrix Antenna" (ARMA) [13]. It is more efficient than the usual Active Electronically Scanned Array, particularly for beam steering up to 60°. To obtain these two different radiation patterns, an X band ARMA [14, 15] was designed with nine active feeding ports inside a matrix built with 5×5 circularly polarized pixels. The weighting functions are applied to the pixels in order to work alternatively in isoflux or directive mode. This paper presents a comparison between theory and experiment on the isoflux mode. Since the directive mode is realized with the same amplitudes and phases, it does not introduce manufacturing problems. Therefore, the demonstrator is only manufactured for the isoflux mode planar antenna as shown in Fig. 1. The article is organized as follows. Section "Antenna" contains a brief antenna description, the S_{ij} measurement setup and a comparison between the simulation and measurement results of the antenna [S] parameters. Section "Experimental device for radiation pattern measurements" describes the experimental device used to feed the antenna with the appropriated weighting functions. This section also presents the [S] parameters measurement of this device. The comparison between simulations and measurements of the whole system (antenna + experimental device) is presented in section "Measurement of the whole device (antenna + experimental device)". Finally, a conclusion is given.

Antenna

Antenna description

The antenna is simulated using CST Microwave Studio and it is depicted in Fig. 1. A square low profile ARMA antenna was built containing 25 pixels [15] with $0.5\lambda_0$ spacing. Only nine are fed by the experimental device. The other ones, located at the edges of the antenna and connected to 50 Ω impedances are not fed. They are only used to maintain a good axial ratio for the whole matrix antenna. Each pixel includes a microstrip patch with four feeding ports, associated with a 90° phase shift, to obtain a circularly polarized field. The polarization circuit is printed on a TMM10i substrate (0.381 mm height) designed to generate these phase shifts. The main challenge to tackle this design is the small area behind the pixel surface ($0.5\lambda_0 \times 0.5\lambda_0 = 18.29$ mm $\times$ 18.29 mm). It must be enough to integrate three hybrid

© Cambridge University Press and the European Microwave Association 2019

CAMBRIDGE UNIVERSITY PRESS

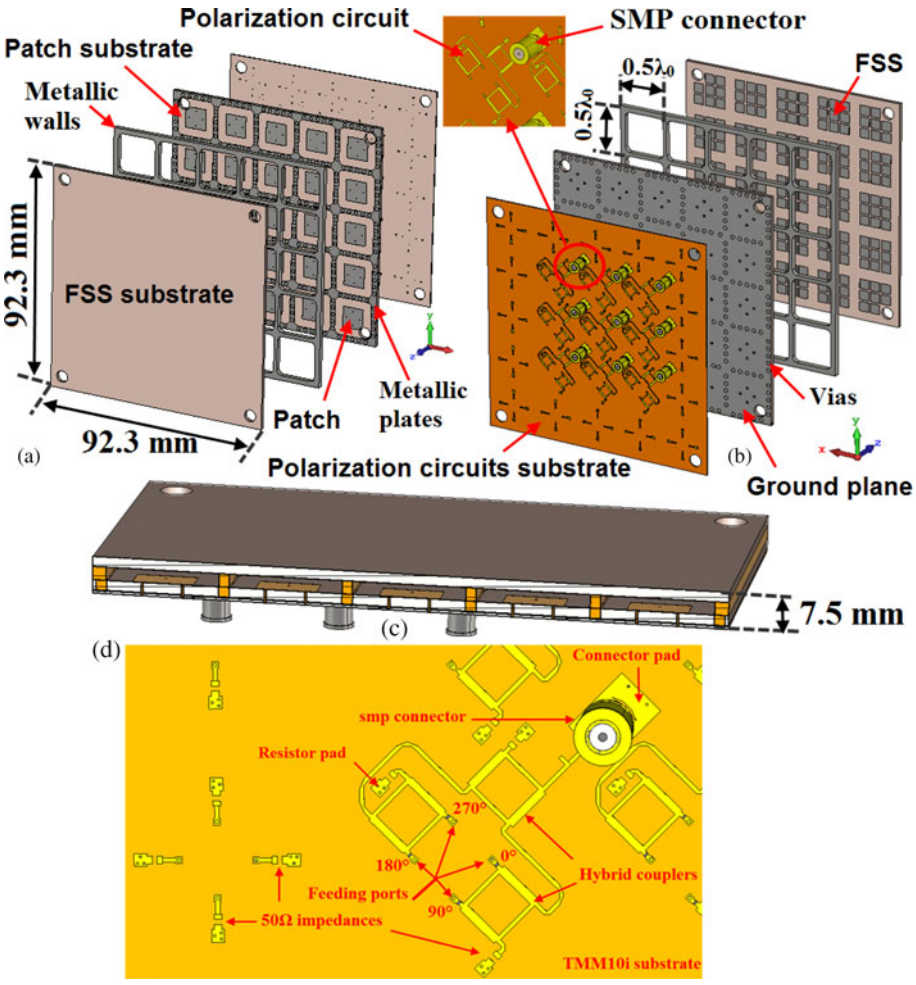


Fig. 1. Low profile circularly polarized ARMA: (a) exploded view of the top to show the radome where the FSS is printed, (b) exploded view of the bottom with the nine polarization circuits, (c) side view to see the low-profile shape, (d) detail of the polarization circuit.

couplers, three resistor pads, and a connector pad (Fig. 1(d)). Each of these three hybrid couplers needs one port connected to a 50 Ω resistor with grounded pads. These pads are designed and optimized separately to minimize their dimensions. SMP connectors are used. The connector pad for grounding and the microstrip line to solder the circuit-connector pin were also optimized to reduce the size. The patches are printed on the top of another substrate (RO6002 laminate, 1.524 mm). They are connected to the outputs of the polarization circuits by plated through holes (PTH). The ground plane is common for both the polarization circuit and the feeding patch substrates. Both substrates are stuck together by a Cuclad 6250 bonding film after removing the bottom metallization of the patch substrate. To connect the metallic walls and the ground plane, metallic plates and PTH are made on the patch layer. The other parts of the metallic walls (2 mm height, 1.5 mm thickness) are connected from the top of the patches substrate to the bottom of the FSS substrate (RO6002 laminate, 1.524 mm).

The manufactured planar antenna is therefore a multilayered structure built with four layers. Figure 2(a) shows the TMM10i substrate used to print the circuit with the nine elements of the RF polarization circuits. The feeding patches are printed on the top of the RO6002 laminate (Fig. 2(b)). Figure 2(c) shows the grid to obtain metallic walls. The FSS printed on the radome is presented in Fig. 2(d).

Scattering matrix measurement setup

A measurement test bench for multi-element antenna, previously described in [16], has been used as shown in Fig. 3. It is equivalent to a multiway VNA (up to 49 ways).

S_{ii} parameters

The frequency evolution of the nine S_{ii} parameters obtained in simulation (Fig. 4(a)) is compared with the experimental one in Fig. 4(b).

In both cases, the curves show the S_{ii} parameters lower than the expected "−10 dB" value on the whole bandwidth, illustrating the capacity of the ARMA solution to work on a wide frequency band [13]. However, the S_{ii} minima are shifted toward high frequencies in the experimental results.

Coupling effects

An important property of the ARMA is that the couplings between the pixels are very small: usually smaller than the ones between elementary antennas in an array [13]. This property is well illustrated in Fig. 5 which shows the modulus of the coupling coefficients between the central port (P5 in Fig. 3) and the other ones for all the frequency range. The experimental results (Fig. 5(b))

https://doi.org/10.1017/S1759078719001004 Published online by Cambridge University Press

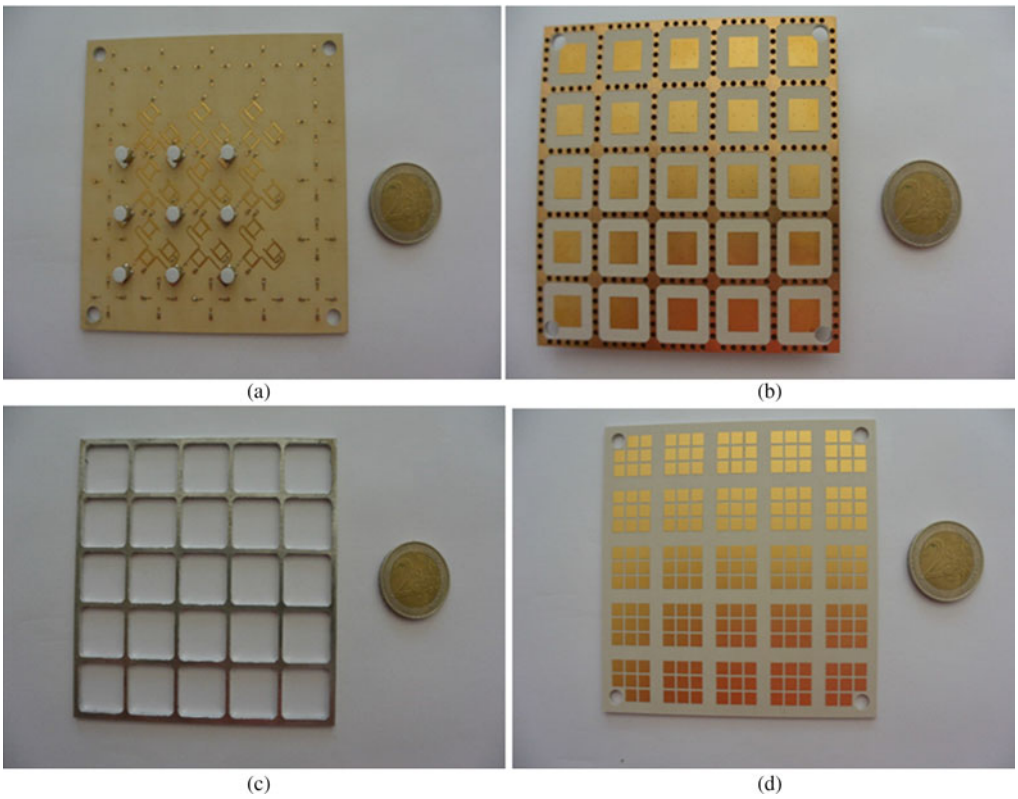


Fig. 2. Multilayer structure: (a) PCB with the nine polarization circuits [14], (b) feeding patches printed on the dielectric substrate, (c) the grid, (d) FSS printed on the radome.

are lower than the theoretical ones (Fig. 5(a)) because the matching impedance losses are increasing this phenomenon, as expected.

Experimental device for radiation pattern measurements

Experimental device description

To measure the directivity, gain, axial ratio, and efficiency, the experimental device includes a power divider function with nine active outputs associated with a table of weightings [14, 15]. The amplitude ratio of all the ports surrounding the central one (level = 1 and phase = 0°) is approximately $A = 0.15$ with a 180° phase. It was not possible to obtain a suitable power divider to check the previous specifications. As a whole, an experimental device was designed for measurements (Fig. 6).

This device is built with "commercial off the shelf components" (COTS). It is made of an equi-amplitude and equi-phase

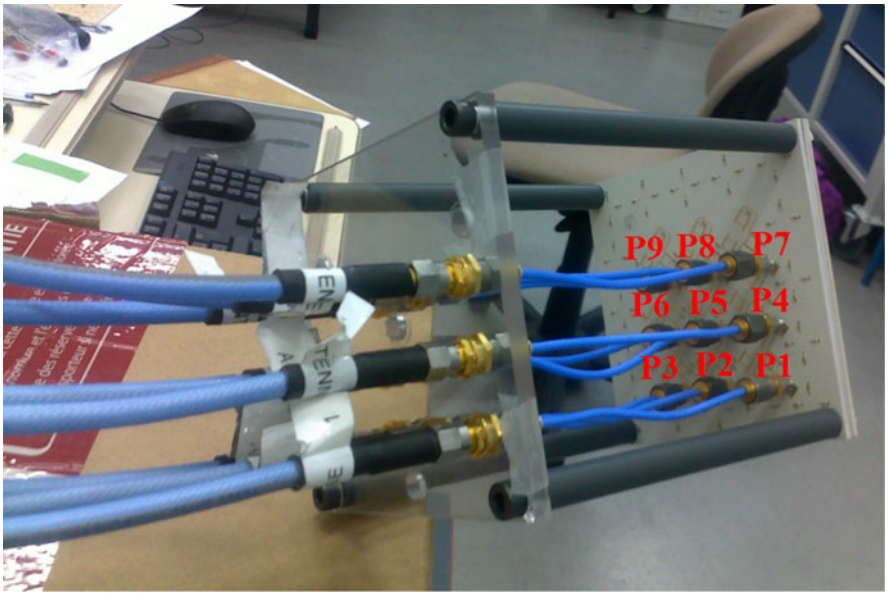


Fig. 3. Experimental setup for S_{ij} measurements.

https://doi.org/10.1017/S1759078719001004 Published online by Cambridge University Press

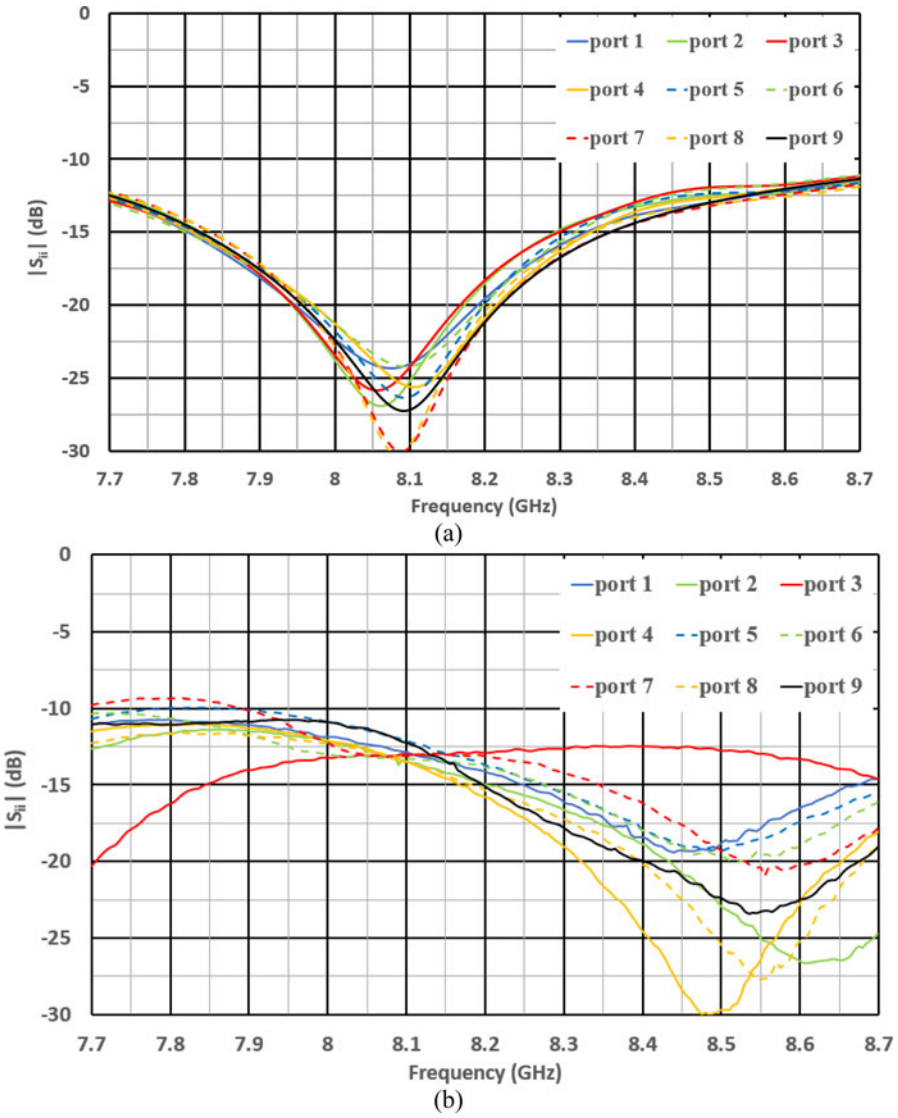


Fig. 4. S_{ii} parameters evolution as a function of the frequency: (a) simulation and (b) experimental results.

power divider with 18 ways. Only nine outputs are used. The other ones are connected to 50 Ω loads, as shown in Fig. 6.

The eight ports corresponding to the pixels surrounding the central one are connected to attenuators to obtain an output level ratio close to $A = 0.15$, as given by the theoretical approach [14, 15].

The central pixel is fed by the central port called P6 through a phase shifter to obtain a 180° phase shift with the surrounding ports. The weighting table obtained experimentally with the device is presented in Table 1 and compared with the theoretical one. The ratio between the central port and the other ones is slightly different ($A = 0.17$) due to the COTS attenuators resolution.

Measured scattering matrix of the experimental device

The previous table of weightings is verified in linear modulus (Fig. 7(a)) and phase (Fig. 7(b)) for the whole frequency range.

The matching parameters S_{ii} are compliant with our −10 dB objective as shown in Fig. 8(a). It is the same for the S_{ij} coupling parameters in Fig. 8(b).

Measurement of the whole device (antenna + experimental device)

The results in this part are compared to the simulation of the antenna in CST Microwave Studio (RF simulator) connected to the measured scattering parameters, integrated in CST Design Studio (circuit simulator).

Isoflux radiation patterns

Radiation patterns (directivity, IEEE gain, and realized gains) are measured in our anechoic chamber (Fig. 9). An aluminum thin sheet allows simulating the nanosat platform. Absorbers were installed behind the antenna to minimize electromagnetic interferences of the motor. Therefore, the back radiation will be minimized resulting in a slight increase of the antenna directivity.

The 3D RHCP radiation pattern theory-measurement comparison is presented at the central frequency of 8.2 GHz in directivity. In Fig. 10(a), the isoflux shape is illustrated on the 3D radiation pattern for theoretical and experimental results. In both cases, the circular symmetry is disturbed by the edges

https://doi.org/10.1017/S1759078719001004 Published online by Cambridge University Press

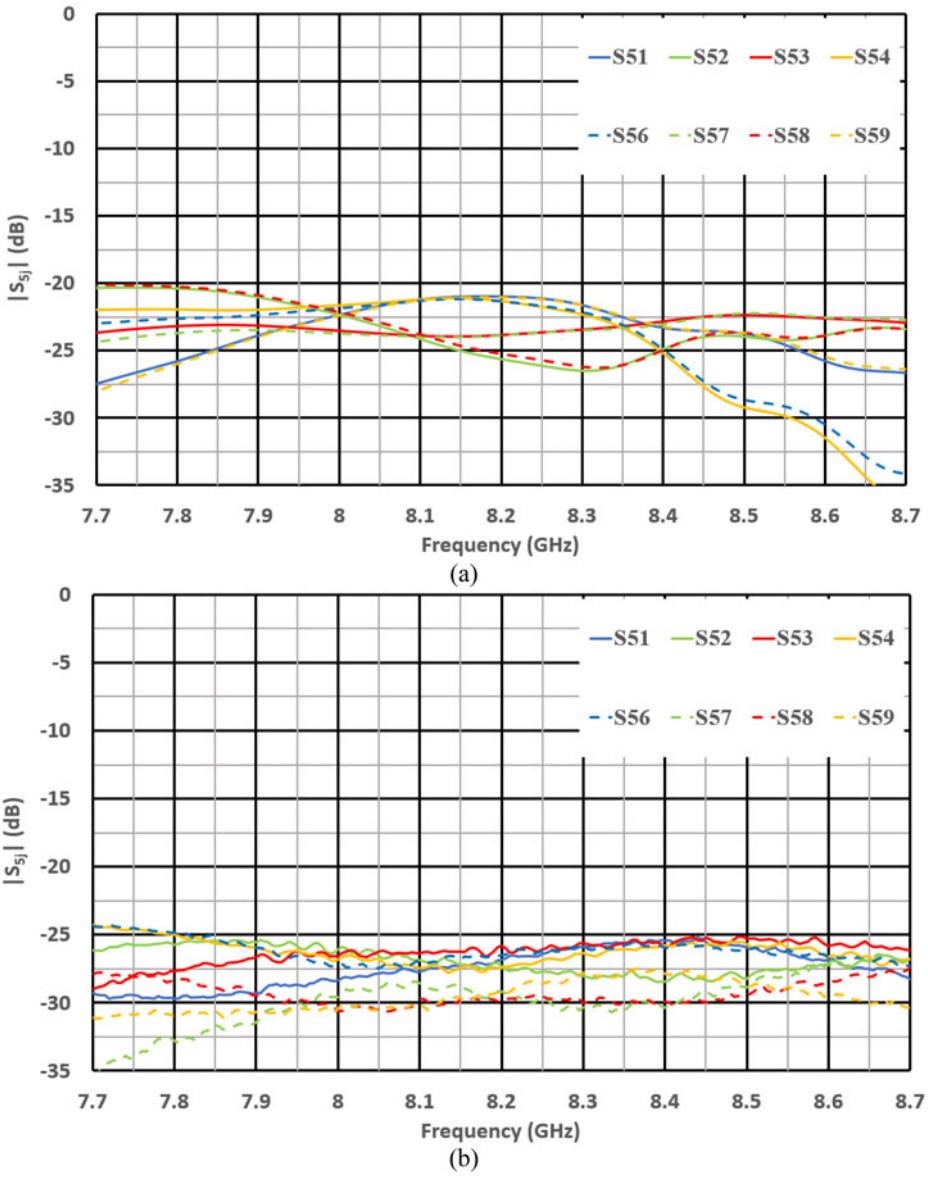


Fig. 5. Mutual couplings between the central pixel and the other ones versus the frequency: (a) theoretical result, (b) experimental result (modulus comparison).

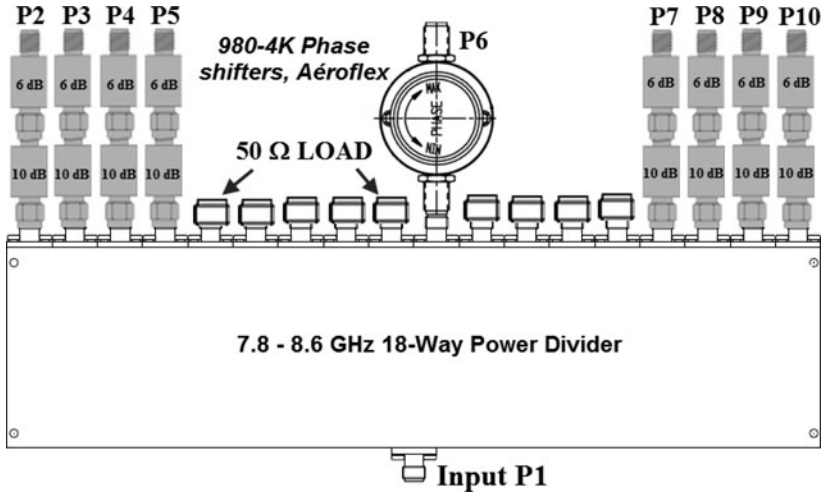


Fig. 6. Experimental device for radiation pattern measurements.

https://doi.org/10.1017/S1759078719001004 Published online by Cambridge University Press

Table 1. The weighting function

	Ideal case	Experimental device
Central pixel level	1.00	0.17
Other pixels level	0.15	0.03
linear ratio	0.15	0.17
Attenuation (dB)	−16.5	−15.2

diffraction. Figure 10(b) gives the RHCP radiation pattern in directivity at the same frequency for some φ cut-planes (0°, 44°, 90°, 134°) and Fig. 10(c) shows the axial ratio versus the θ site angle: the results are not really compliant with the isoflux characteristics around the axial direction. However, it is not a problem for a spatial bi-mode application [14, 15] because the isoflux solution is used only for angles higher than 30°.

A good agreement is obtained between the theoretical and experimental results.

Frequency dependence comparison and power balance interpretation

Figure 11 shows the theoretical and experimental evolution with the frequency of the directivity and associated maximum realized gain. The theoretical and experimental results are in good agreement on the whole frequency band.

The directivity is obviously higher than the realized gain (about 7 versus −10 dBi) due to the losses of our experimental device. This one introduces 14.4 dB losses, as shown in Table 1: $10\log(0.17^2 + 8\times 0.03^2)$. It remains 2.6 dB due to the losses in the antenna itself (50 Ω resistances, dielectric substrates, transmission lines, connectors, etc.) and due to the experimentation process (±0.8 dB).

Conclusion

After describing the ARMA theoretical approach from [14, 15] to obtain a bimode Earth coverage from small satellites on LEO orbit, an ARMA antenna was manufactured to validate the solution. A comparison between theory and experiment on the isoflux

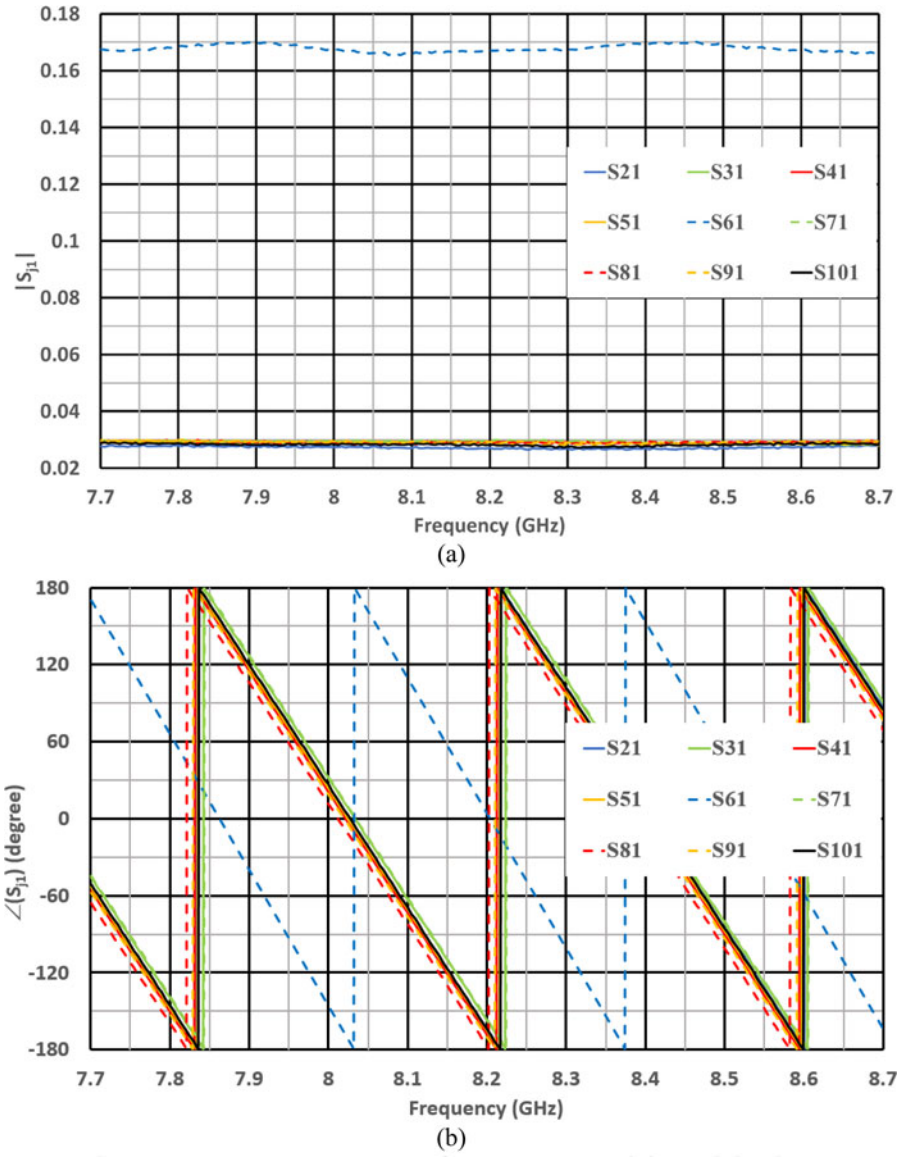


Fig. 7. Input–output parameters versus frequency: (a) modulus and (b) phase.

https://doi.org/10.1017/S1759078719001004 Published online by Cambridge University Press

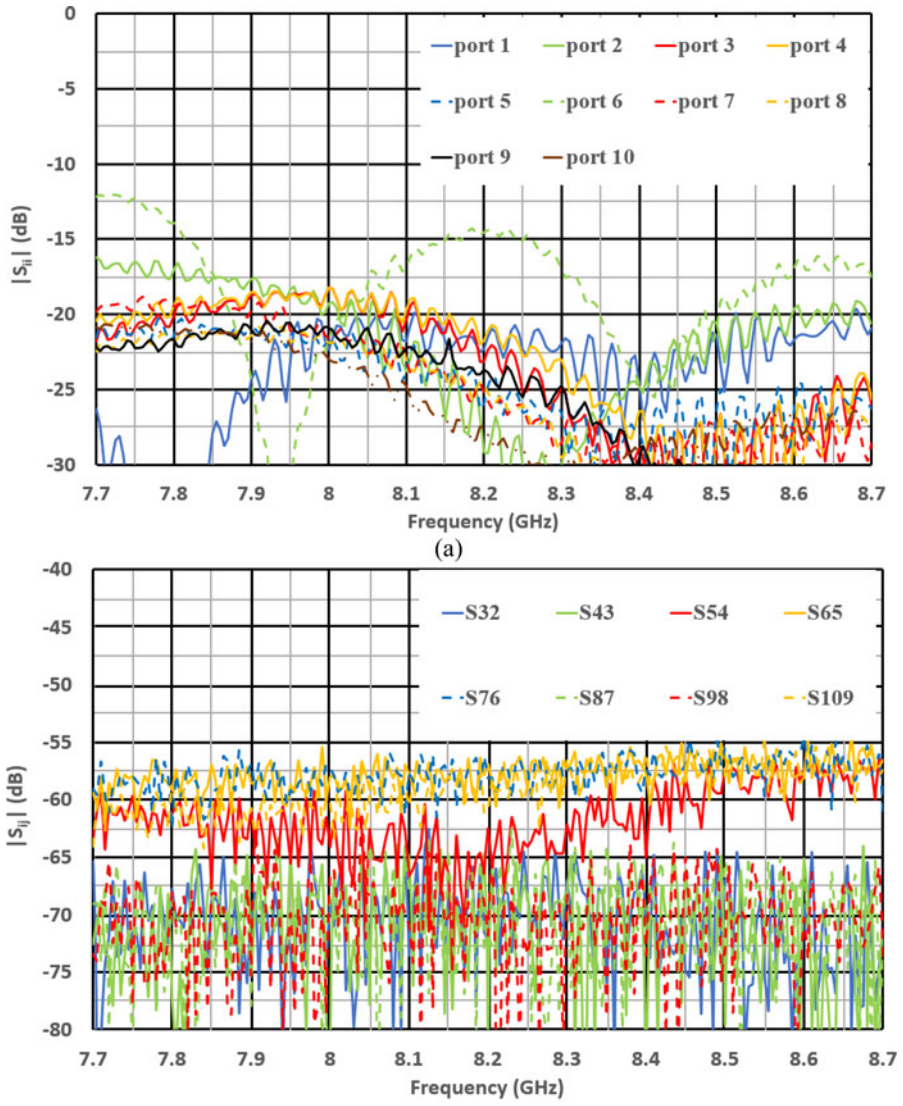


Fig. 8. (a) S_{ii} and (b) S_{ij} parameters evolution over the frequency range.

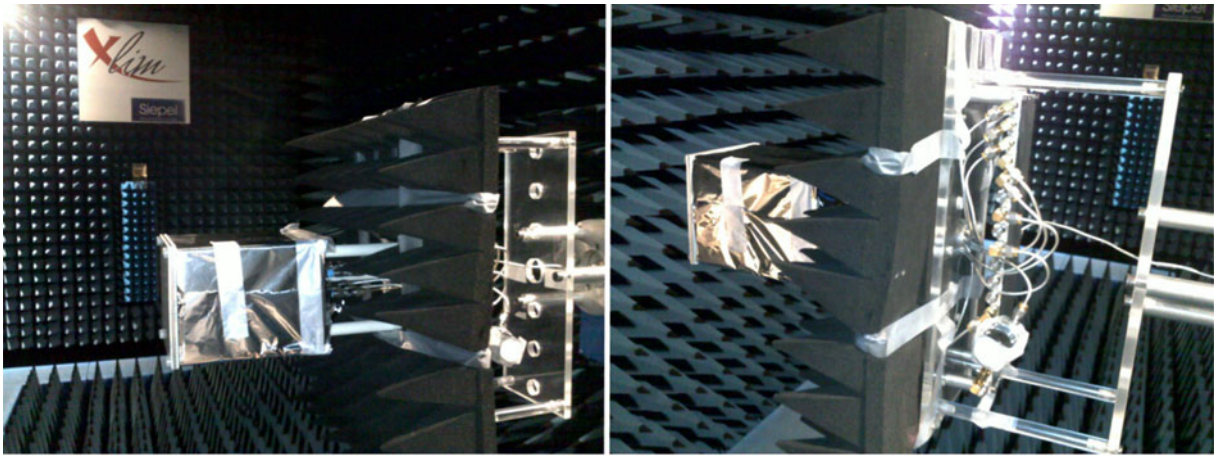


Fig. 9. XLIM anechoic chamber used for radiation patterns measurement : (a) side view, (b) back view.

https://doi.org/10.1017/S1759078719001004 Published online by Cambridge University Press

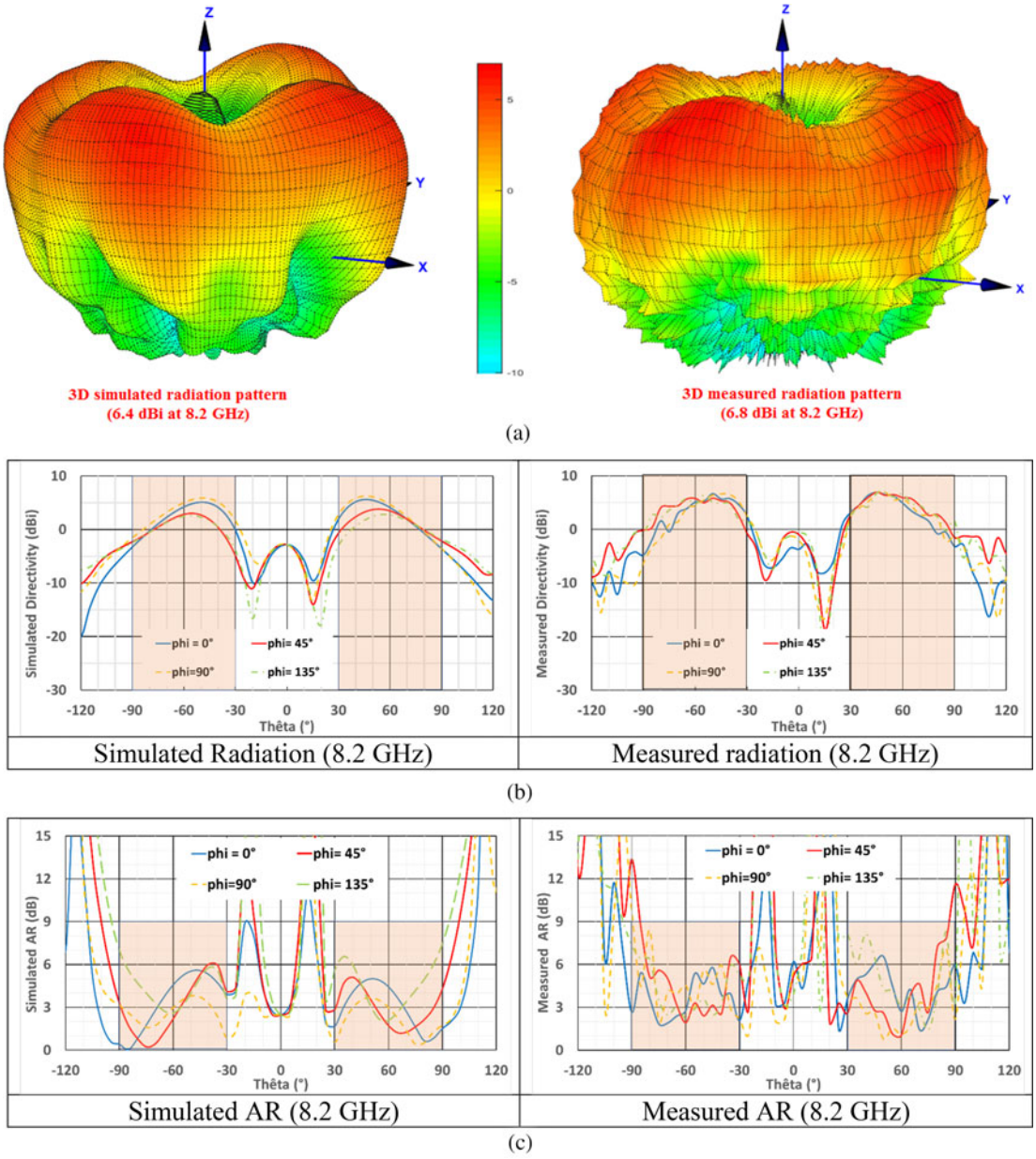


Fig. 10. (a) 3D radiation patterns, (b) RHCP radiation pattern in $\varphi = 0°$, 44°, 90°, and 134° cut-planes, (c) axial ratio for the same cut-planes.

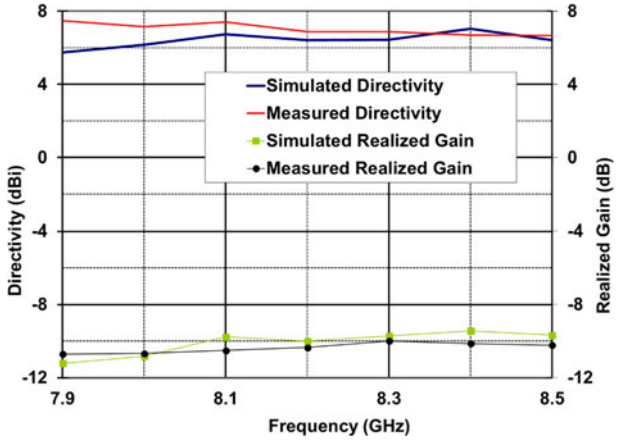


Fig. 11. Theoretical and experimental directivity and maximum realized gain versus frequency.

mode (the axial mode does need not to be validated) in the X frequency band has been performed. The results are in good agreement to show that the manufacturing problems are controlled in this frequency band.

Acknowledgement. The authors would like to thank the French Space Agency – CNES (Centre National d'Etudes Spatiales) – FRANCE for their financial support to this study.

References

1. **Geyer H** (1966) Runder Hornstrahler mit ringformigen Sperrtopfen zur gleichzeitigen Ubertragung zweier polarisationsentkoppelter Wellen. *Frequenz* **20**, 22–28 (especially p. 27).
2. **LaGrone A and Roberts G** (1966) Minor lobe suppression in a rectangular horn antenna through the utilization of a high impedance choke flange. *IEEE Transactions on Antennas and Propagation* **14**, 102, 104.

https://doi.org/10.1017/S1759078719001004 Published online by Cambridge University Press

3. **Wohlleben R, Mattes H and Lochner O** (1972) Simple small primary feed for large opening angles and high aperture efficiency. *Electronics Letters* **8**, 474, 476.
4. **Shafai L** (1977) Broadening of primary feed patterns by small E-plane slots. *Electronics Letters* **13**, 102–103.
5. **Brachat P** (1994) Sectoral pattern synthesis with primary feeds. *IEEE Transactions on Antennas and Propagation* **42**, 484–491.
6. **Arnaud E, Menudier C, Fouany J, Monediere T and Thevenot M** (2017) X-band compact dual circularly polarized isoflux antenna for nanosatellite applications. *International Journal of Microwave and Wireless Technologies* **9**, 1509–1516.
7. **Maldonadoa AR, Panduroa MA, del Rio Bociob C and Mendez A** (2013) Design of concentric ring antenna array for a reconfigurable isoflux pattern. *Journal of Electromagnetic Waves and Applications* **27**, 1483–1495.
8. **Maldonadoa AR, Panduroa MA, del Rio Bociob C and Mendez A** (2011) Design of concentric ring antenna arrays for isoflux radiation in GEO satellites. *Journal of IEICE Electronics Express* **8**, 484–490.
9. **Jin J, Wang HL, Zhu WM and Liu YZ** (2006) Array patterns synthesizing using genetic algorithm. *Progress in Electromagnetics Research Symposium, Cambridge, USA*, 26–29 March 2006.
10. **Ibarra M, Reyna A, Panduro MA and del Rio-Bocio C** (2011) Design of aperiodic planar arrays for desirable isoflux radiation in GEO satellites. *Antennas and Propagation (APSURSI), Spokane*.
11. **Quijano JLA, Righero M and Vecchi G** (2014) Sparse 2-D array placement for arbitrary pattern mask and with excitation constraints: a simple deterministic approach. *IEEE Transactions on Antennas and Propagation* **62**, 1652–1662.
12. **Roy SM and Balbin I** (2010) Handheld reader antenna at 5.8 GHz. *Department of Electrical and Computer Systems Engineering, Monash University, Clayton, Victoria, Australia*.
13. **Jecko B, Arnaud E, Abou Taam H and Siblini A** (2017) The ARMA concept: comparison of AESA and ARMA technologies for agile antenna design. *FERMAT* **20**, Article 2.
14. **Siblini A, Jecko B and Arnaud E** (2017) Multimode reconfigurable nanosatellite antenna for PDTM application. *2017 11th European Conference on Antennas and Propagation (EUCAP), Paris*, pp. 542–545.
15. **Siblini A, Taam HA, Jecko B, Ramma M, Bellion A and Arnaud E** (2017) ARMA feeding techniques for isoflux coverage from a micro satellite. *Advances in Science, Technology and Engineering Systems Journal* **2**, 63–69.
16. **Menudier C, Arnaud E, Thevenot M, Fezai F, Oueslati A, Chevalier N, Reynaud S and Monediere T** (2015) Synthesis of multi-element antennas using a measurement test bench. *2015 European Radar Conference (EuRAD), Paris*, pp. 345–348.



Eric Arnaud was born in France in 1970. He received the Diplôme D'Etudes Supérieures Specialisées (DESS) and the Ph.D. degrees in Electronics and Telecommunication from the University of LIMOGES in 1994 and 2010, respectively. He did his Ph.D. on circularly polarized EBG antenna. From 1996 to 2001, he has been in charge of the Microwave part of Free-Electron Laser (L.U.R.E). Since 2001, he has been in charge of XLIM laboratory's antenna test range. He participated in several research projects related to the design, development, and characterization of antennas. His research interests are mainly in the fields of circularly polarized EBG antenna, agile electromagnetic band gap matrix antenna, and isoflux pattern antenna.



A. Siblini, Doctor in telecommunication, high-frequency systems, and agile antenna design during "Cotutelle PhD program" between the Lebanese University and Limoges University/ France 2017. Masters in electronics and signal processing from Lebanese University 2012. Telecommunication engineering from Lebanese University 2011. Instructor and researcher at Lebanese International University Lebanon LIU. Researcher at Lebanese University



Anthony Bellion received his Engineer Diploma in Electronics in 2003 from the Ecole Nationale Superieure d'Ingénieurs de Limoges (ENSIL) (Limoges, France). He received his Ph.D. degree in Optical Communication and Microwave Techniques from the University of Limoges, Limoges, France in 2008 working on multi polarizations and UWB antenna designs for direction finding systems. After industrial experience with Thales, France, he joined the Antenna Department of the French Space Agency (CNES). Since 2016, he has headed the CNES Antenna Department. His areas of research are mainly UWB antennas, miniature antennas design, and characterization.



B. Jecko was born in Trélissac (24), France in 1944. He obtained the Ph.D. degree in Physics from the University of Limoges (France) in 1979. In this university, he served as a professor (exceptional class in 2000) at the IUT (GE teaching department founder in Brive in 1985). In the research area, he was first an electromagnetism specialist for EMC (fellow member EMP) and now for Telecommunications, Radar, and Electronic Warfare applications. He created and headed the department OSA at the XLIM institute (University of Limoges – CNRS laboratory) until 2009. In 2009, he was appointed as a DRRT (Regional Delegate for Research and Technology) by the French Research Ministry until his retirement in September 2013. Since then, he is coming back to his research department as an Emeritus Professor. Publications ≅ 130, Communications ≅ 400, Patents ≅ 30, Thesis supervision ≅ 130 – HDR ≅ 7

https://doi.org/10.1017/S1759078719001004 Published online by Cambridge University Press